

Supporting Information

Inclusion Crystals as Vapochromic Chemosensors: Fabrication of a Mini-sensor Array for Discrimination of Small Aromatic Molecules based on Side-Chain Engineering of Naphthalenediimide Derivatives

Toshikazu Ono,* Yoshifumi Tsukiyama, Sou Hatanaka, Yuma Sakatsume, Tomoki Ogoshi, and Yoshio Hisaeda*

Fig. S1 ^1H -NMR spectra of **2** in DMSO- d_6 .

Fig. S2 ^{13}C -NMR spectra of **2** in CDCl₃.

Fig. S3 ^1H -NMR spectra of **3** in Acetone- d_6 .

Fig. S4 ^{13}C -NMR spectra of **3** in CDCl₃.

Fig. S5 Photographs of **2** and **2**•guest in day light (upper row) and UV-light irradiation (bottom row).

Fig. S6 Photographs of **3** and **3**•guest in day light (upper row) and UV-light irradiation (bottom row).

Fig. S7 Diffuse reflectance spectra of **1** and **1**•guest.

Fig. S8 Diffuse reflectance spectra of **2** and **2**•guest.

Fig. S9 Diffuse reflectance spectra of **3** and **3**•guest.

Fig. S10 Summary of diffuse reflectance spectra of **1–3** with vapors.

Fig. S11 Photoluminescence quantum yields of **1–3** (guest free), **1**•guest, **2**•guest, and **3**•guest. Excitation at 370 nm.

Table S1 Calculated concentrations of vapor analytes in the chamber.

Table S2 Preparation of toluene vapor

Table S3 Preparation of *p*-Xylene vapor

Fig. S12 Schematic illustration of experimental setup.

Fig. S13 Crystal structure of **1**.

Fig. S14 Crystal structure of **1**•toluene.

Fig. S15 Crystal structure of **1**•*p*-xylene.

Fig. S16 Crystal structure of **1**•4-fluorotoluene.

Fig. S17 Crystal structure of **1**•anisole.

Fig. S18 Crystal structure of **2**•toluene.

Fig. S19 Crystal structure of **2**•2,5-dimethylfuran.

Fig. S20 PXRD **1** and **1**•guest.

Fig. S21 PXRD **2** and **2**•guest.

Fig. S22 PXRD **3** and **3**•guest.

Fig. S23 TG of **1**•toluene.

Fig. S24 TG of **1**•*p*-xylene.

Fig. S25 TG of **1**•4-fluorotoluene.

Fig. S26 TG of **1**•anisole.

Fig. S27 TG of **2**•toluene.

Fig. S28 TG of **2**•2,5-dimethylfuran.

Fig. S29 TG of **1**•toluene.

Fig. S30 TG of **1**•*p*-xylene.

Fig. S31 TG of **1**•4-fluorotoluene.

Fig. S32 TG of **1**•anisole.

Fig. S33 Sorption isotherms of **1** toward (a) toluene and (b) benzene vapors.

Fig. S34 Guest inclusion determined by $^1\text{H-NMR}$.

Fig. S35 Comparison of diffuse reflectance spectra of **1** and **4** with vapors.

Fig. S36 Comparison of normalized emission spectra of **1** and **4** with vapors.

Fig. S37 Photoluminescence quantum yields of **1**, **4**, **1**•guest, and **4**•guest. Excitation at 370 nm.

Fig. S38 Calculated HOMO-LUMO levels of the guest molecules and **1**.

Fig. S39 Calculated HOMO-LUMO levels of **1-3** (orbital contour value 0.036).

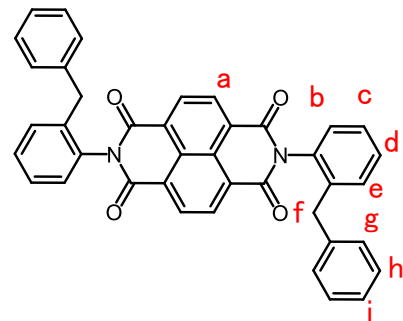
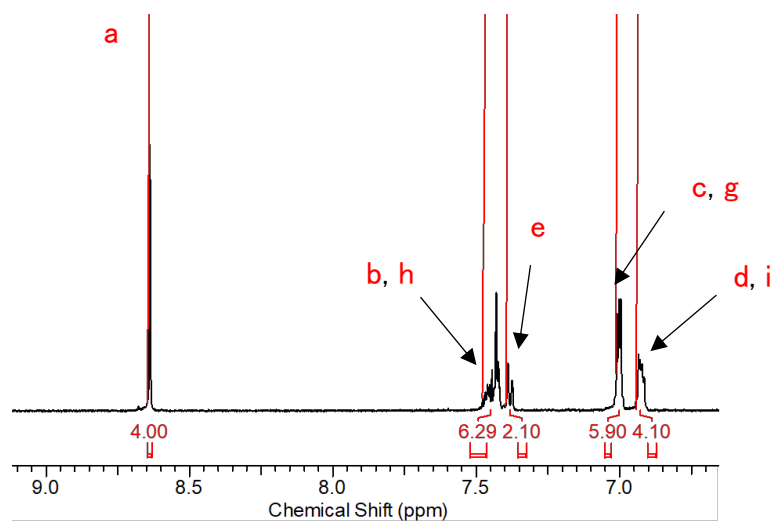
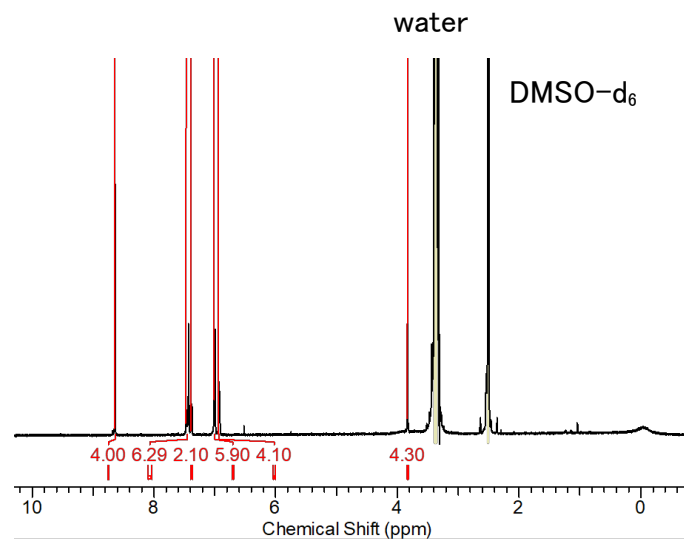


Fig. S1 ^1H -NMR spectra of **2** in $\text{DMSO}-d_6$.

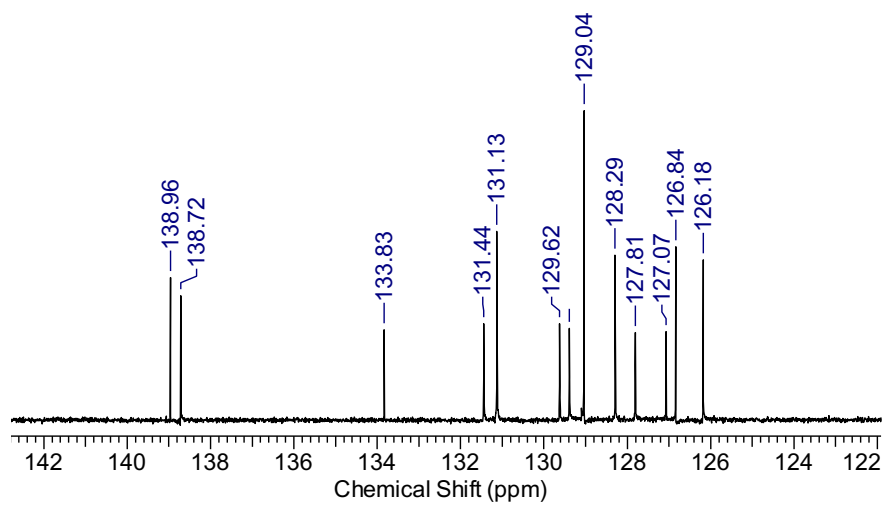
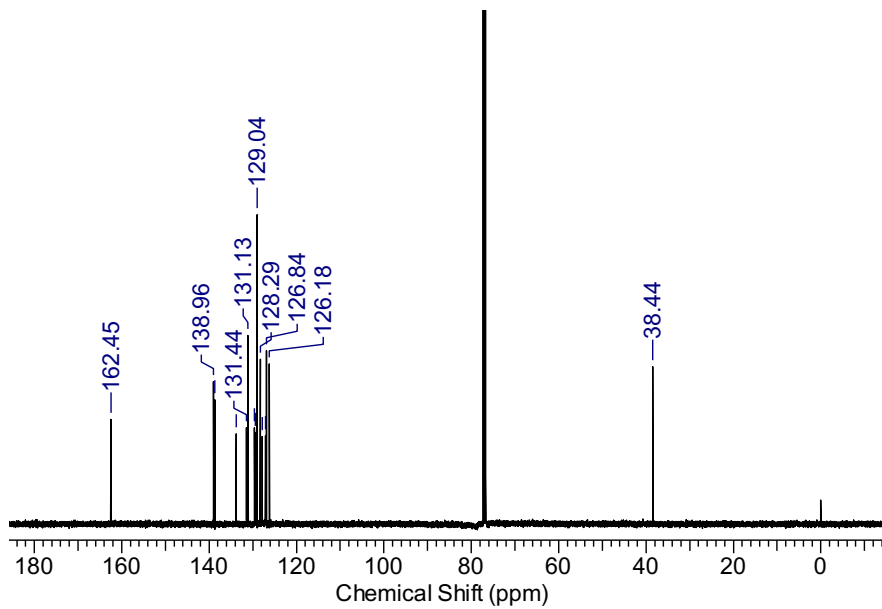


Fig. S2 ^{13}C -NMR spectra of **2** in CDCl_3 .

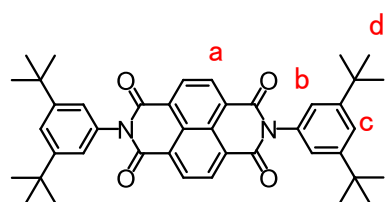
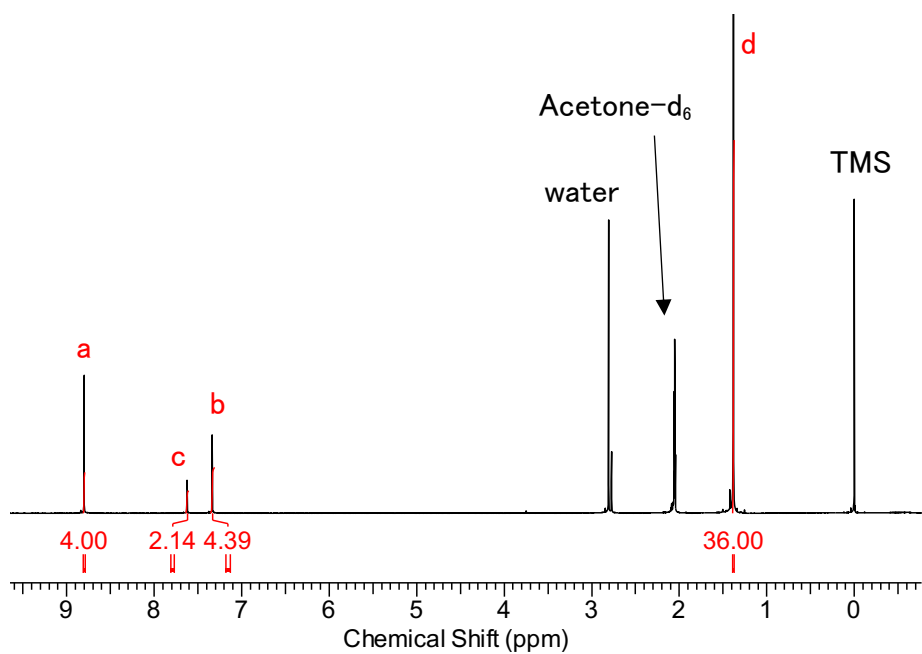


Fig. S3 ^1H -NMR spectra of **3** in Acetone- d_6 .

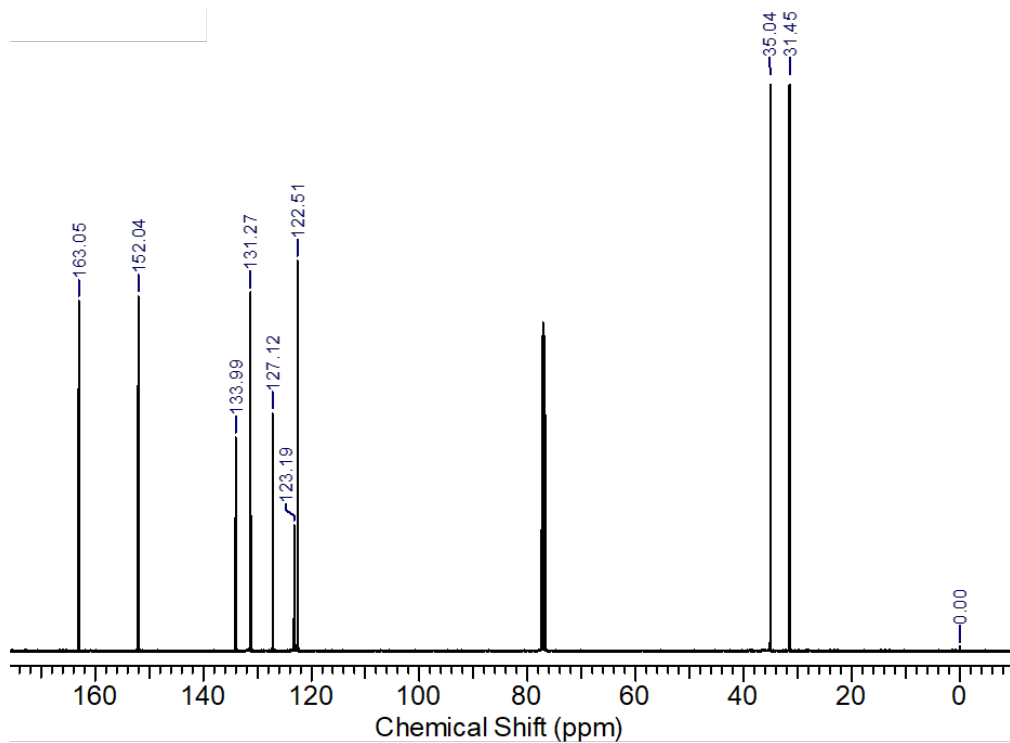


Fig. S4 ^{13}C -NMR spectra of **3** in CDCl_3 .

Sensing ability of 2 and 3 in the solid-states in response vapors.

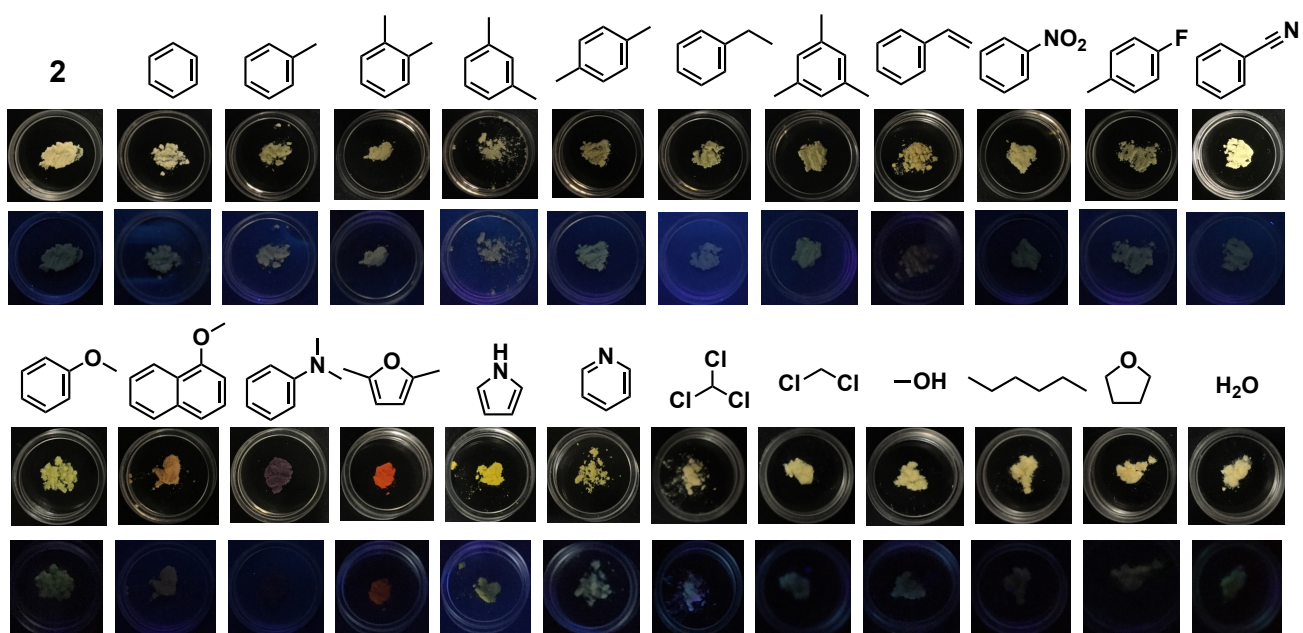


Fig. S5 Photographs of **2** and **2**•guest in day light (upper row) and UV-light irradiation (bottom row).

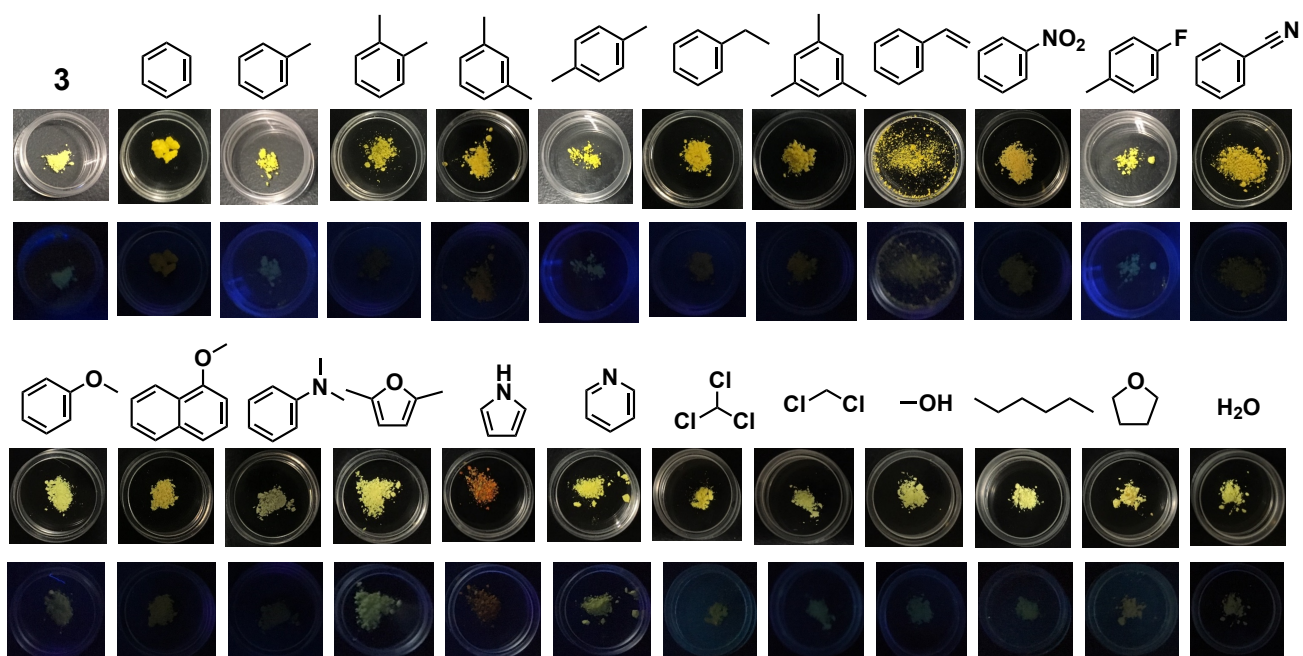


Fig. S6 Photographs of **3** and **3**•guest in day light (upper row) and UV-light irradiation (bottom row).

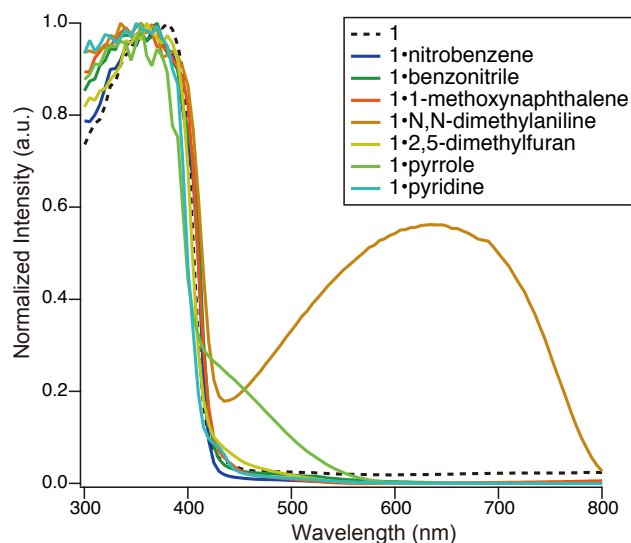
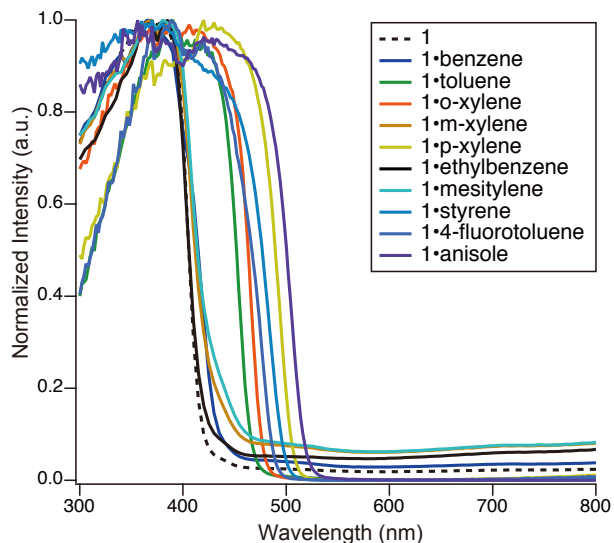


Fig. S7 Diffuse reflectance spectra of **1** and **1**•guest.

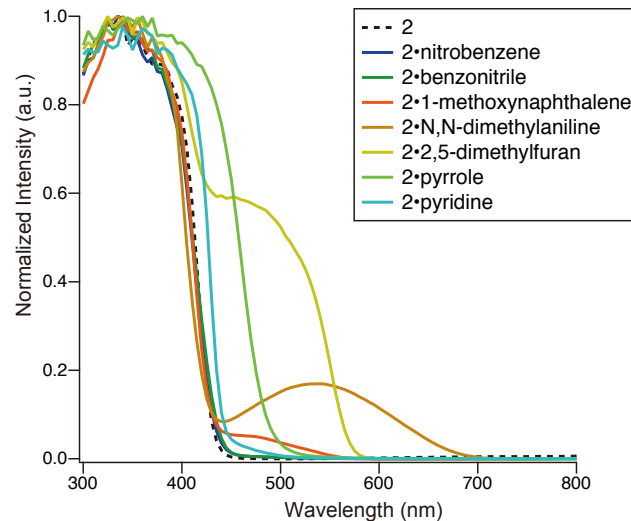
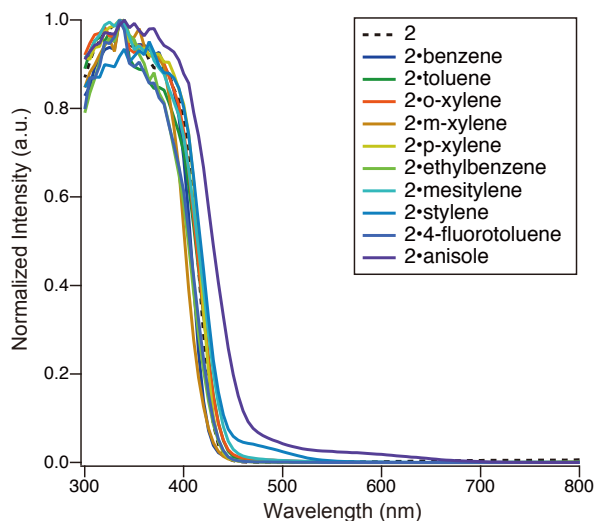


Fig. S8 Diffuse reflectance spectra of **2** and **2**•guest.

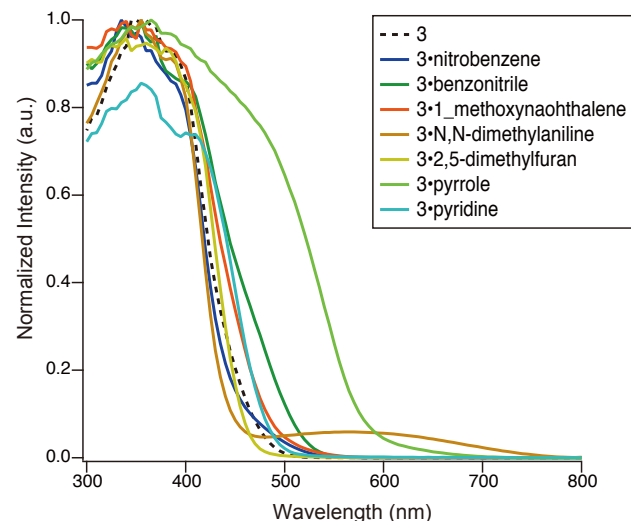
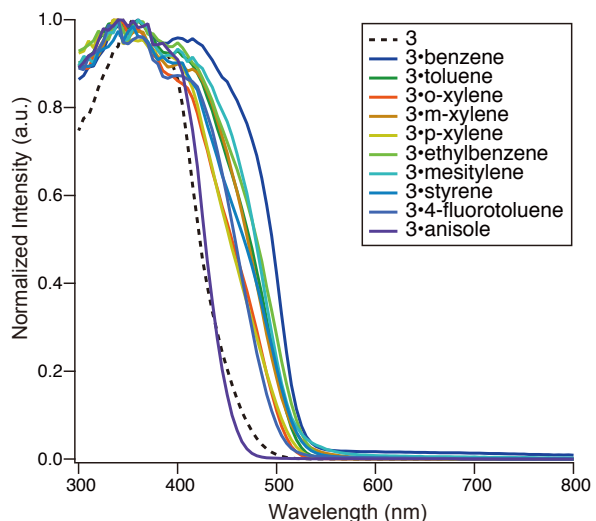


Fig. S9 Diffuse reflectance spectra of **3** and **3**•guest.

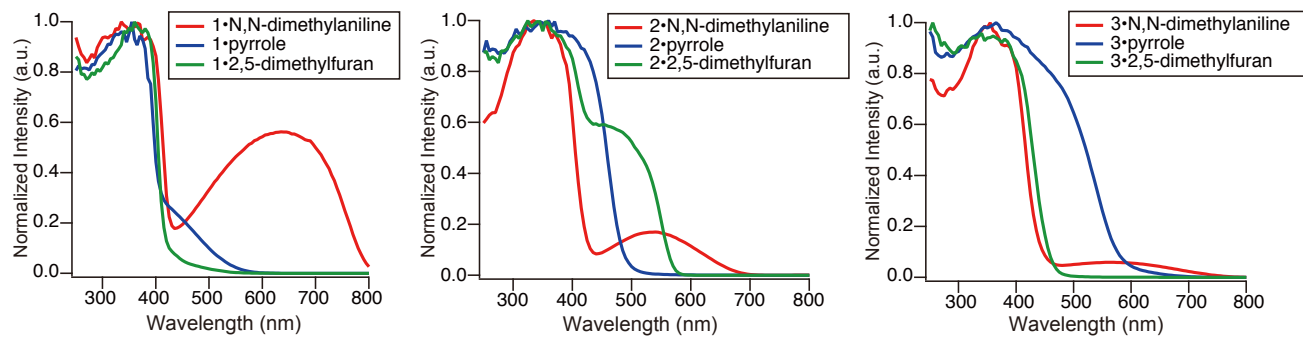


Fig. S10 Summary of diffuse reflectance spectra of **1–3** with vapors.

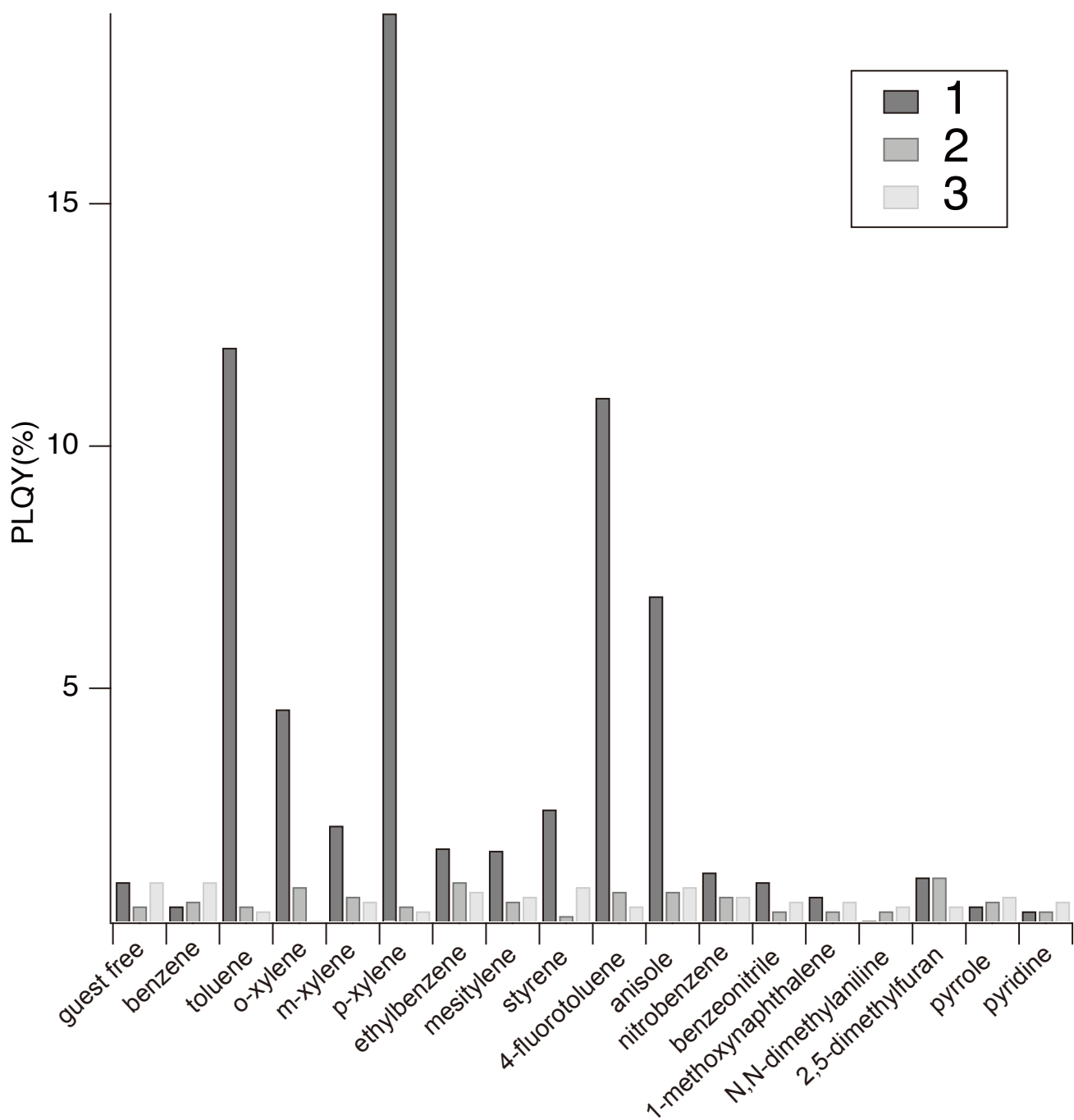


Fig. S11 Photoluminescence quantum yields of **1–3** (guest free), **1•guest**, **2•guest**, and **3•guest**. Excitation at 370 nm.

Table S1 Calculated concentrations of vapor analytes in the chamber.

Guest	Saturated vapor pressure at 25°C (Pa) [*]	ppm in the sample tube
benzene	12700	50859
toluene	3790	15177
ethylbenzene	1270	5126
<i>o</i> -xylene	880	3524
<i>m</i> -xylene	1130	4525
<i>p</i> -xylene	1190	4765
1,3,5-trimethylbenzene	330	1321
styrene	810	3243
nitrobenzene	30	120
<i>p</i> -fluorotoluene	3000	12014
benzonitrile	110	441
anisole	472	1890
1-methoxynaphthalene	3.999**	16
<i>N,N'</i> -dimethylaniline	46***	184
2,5-dimethylfuran	30010****	120180
pyrrole	1100	4405
pyridine	2760	11052
chloroform	26200	104923
dichloromethane	58200	233073
methanol	16900	67679
hexane	20200	80894
tetrahydrofuran	21600	86501
water	3170	12694

* CRC Handbook of Chemistry and Physics, 76th Edition.

** 30°C : A. Das, K. K. Mahato, T. Chakraborty, *J. Chem. Phys.*, **2001**, *114*, 8310-8315.

***20°C : E. P. Fleming, T. C. Fitt, *Industrial and Engineering Chemistry*, **1950**, *42*, 2253-2258.

****58°C : A. Mejía, H. Segura, M. Cartes, J. A. P. Coutinho, *J. Chem. Eng. Data*, **2012**, *57*, 2681–2688.

Preparation of toluene and *p*-xylene vapor phase.

Toluene or *p*-xylene vapor was prepared by heating the pure solvents in a sealed vial (100 mL). The vapor concentrations were obtained according to the following equation:

$$C = \frac{\rho V}{V_0}$$

C: Vapor concentration (ppm), ρ : density of pure reagents (g/cm^3), V : volume of pure reagents solution (μL), V_0 : system volume (L).

Table S2 Preparation of toluene vapor

Reagents	ρ (g/cm^3)	C (ppm)	V (μL)
toluene	0.8669	50	5.8
	0.8669	20	2.3
	0.8669	10	1.1

Table S3 Preparation of *p*-Xylene vapor

Reagents	ρ (g/cm^3)	C (ppm)	V (μL)
<i>p</i> -xylene	0.86	100	11.6
	0.86	50	5.8
	0.86	20	2.3

Time course of sensor (**1**) response in solid matrices.

The closed atmosphere was designed by using a quartz fluorescence cell in which **1** powder (c.a. 500 µg) paste onto a filter paper (1 cm × 1.5 cm) were placed. The **1** was exposed to one drop (50 µL) of guest at the bottom of the cell, which was then capped. Soon after the fluorescence was monitored.

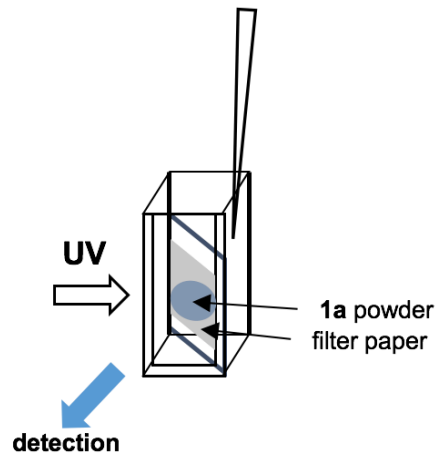


Fig. S12 Schematic illustration of experimental setup.

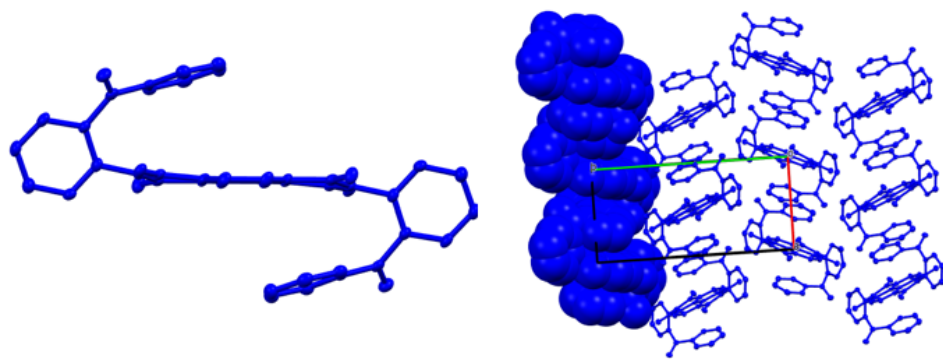


Fig. S13 Crystal structure of **1**. The ellipsoids are plotted at the 50% probability level, and the space-filling models are also included.

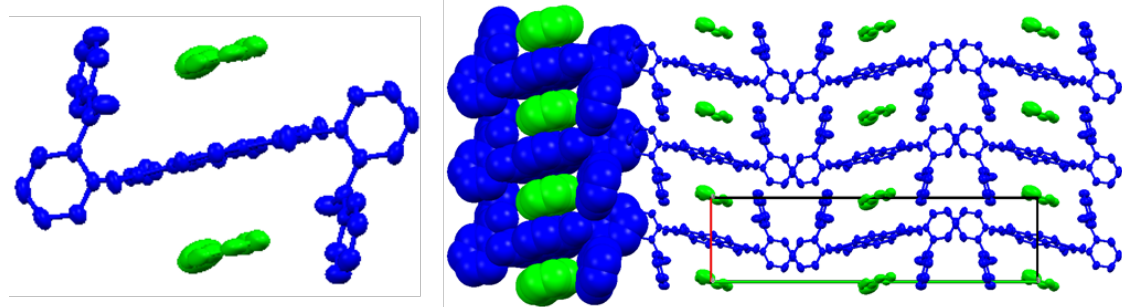


Fig. S14 Crystal structure of **1**·toluene. Blue: **1**, Light green; toluene. In this crystal structure, the guest toluene molecules are disordered. The ellipsoids are plotted at the 50% probability level, and the space-filling models are also included.

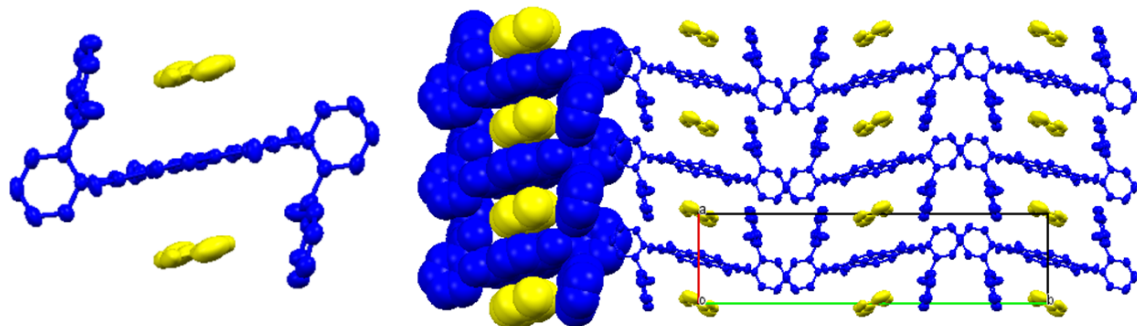


Fig. S15 Crystal structure of **1**·*p*-xylene. Blue: **1**, Yellow; *p*-xylene. The ellipsoids are plotted at the 50% probability level, and the space-filling models are also included.

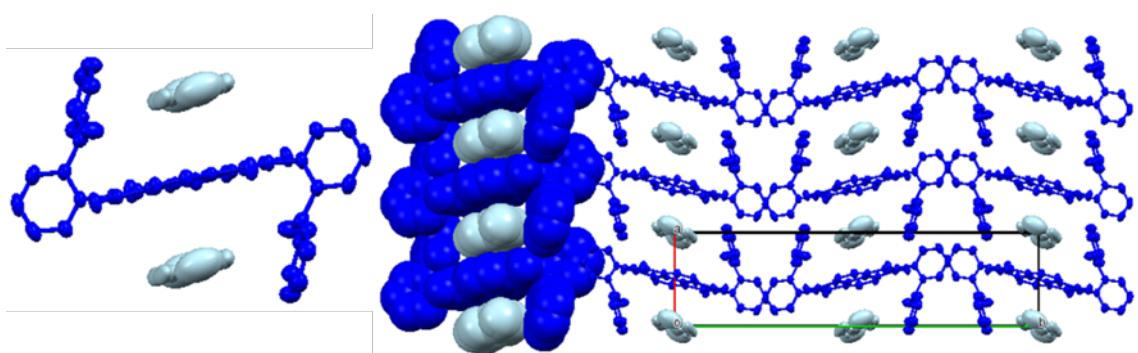


Fig. S16 Crystal structure of **1**⊃4-fluoroyoluene. Blue: **1**, Light blue; 4-fluorotoluene. In this crystal structure, the guest 4-fluorotoluene molecules are disordered. The ellipsoids are plotted at the 50% probability level, and the space-filling models are also included.

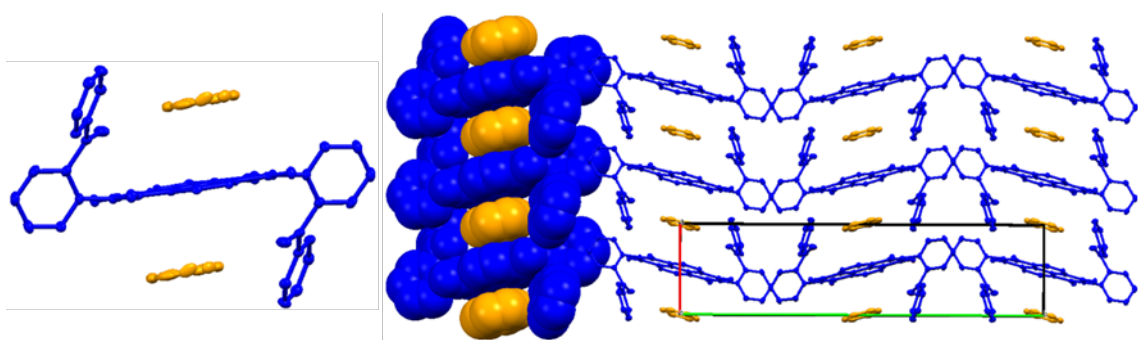


Fig. S17 Crystal structure of **1**⊃anisole. Blue: **1**, Orange; anisole. In this crystal structure, the guest anisole molecules are disordered. The ellipsoids are plotted at the 50% probability level, and the space-filling models are also included.

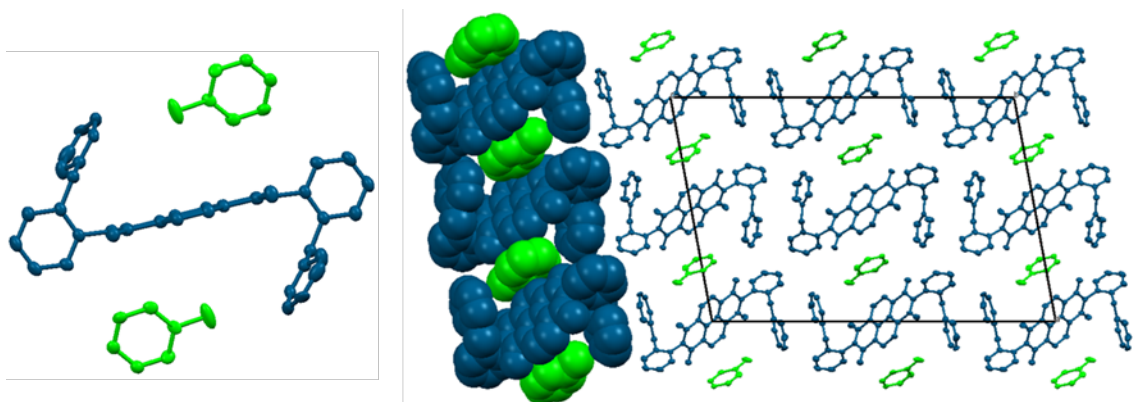


Fig. S18 Crystal structure of **2**⊃toluene. Dark Blue: **2**, Light green; toluene. The ellipsoids are plotted at the 50% probability level, and the space-filling models are also included.

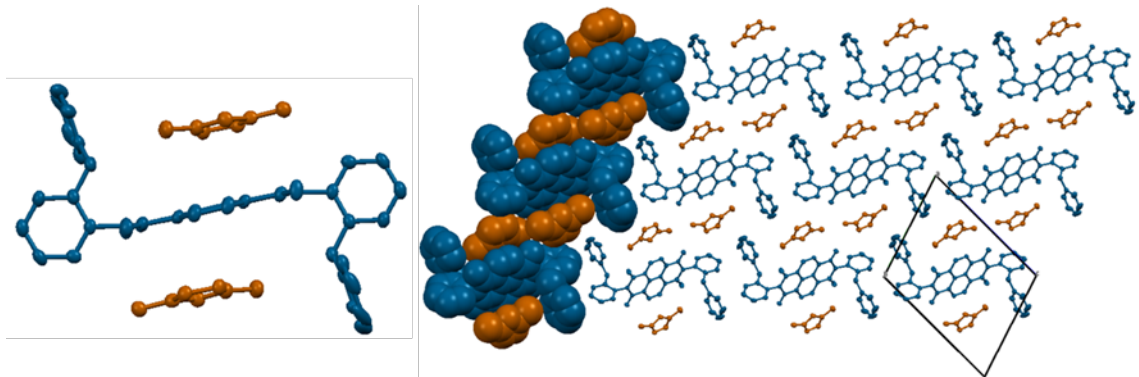


Fig. S19 Crystal structure of **2**•2,5-dimethylfuran. Dark Blue: **2**, Brown: 2,5-dimethylfuran. The ellipsoids are plotted at the 50% probability level, and the space-filling models are also included.

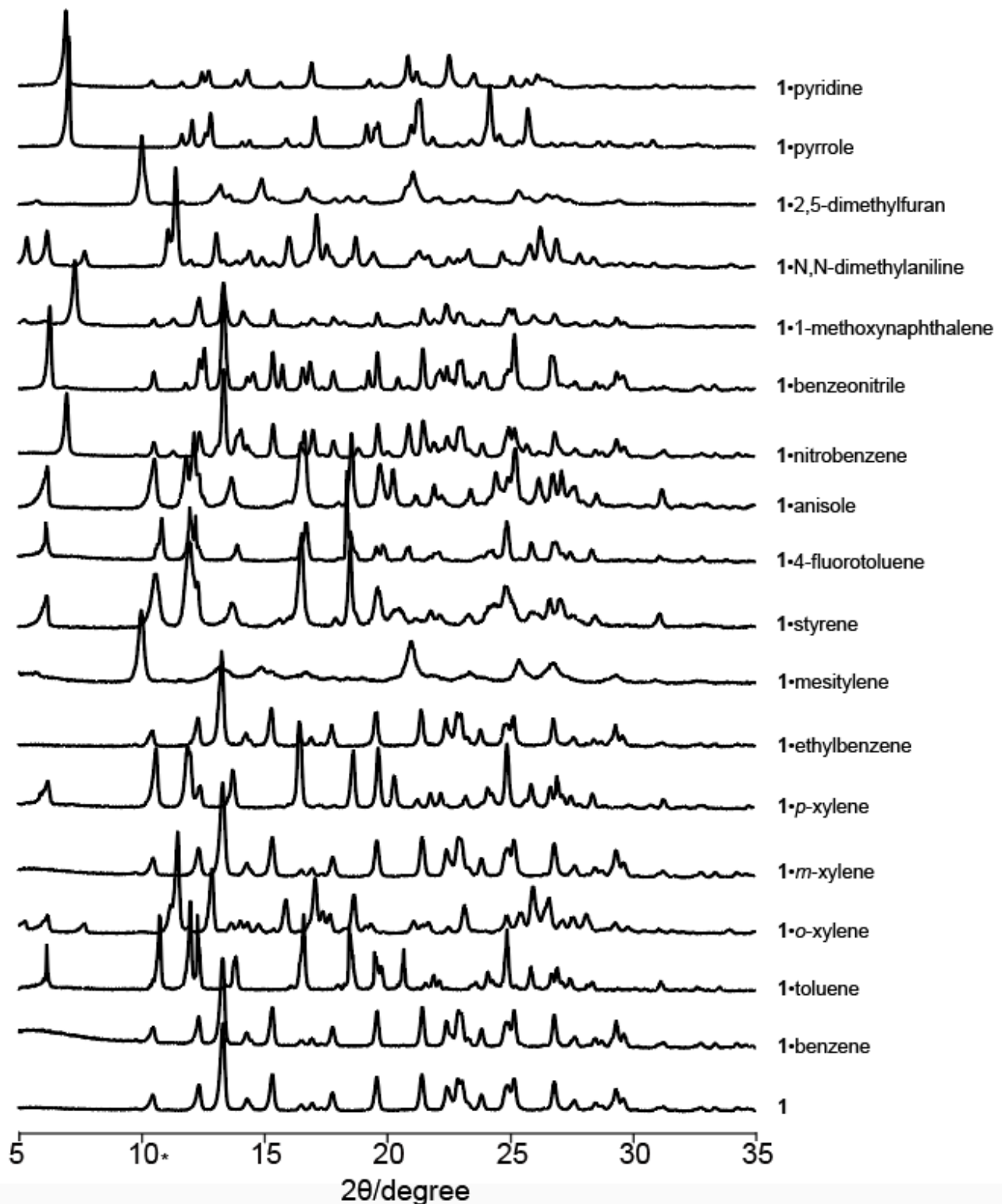


Fig. S20 PXRD 1 and 1•guest.

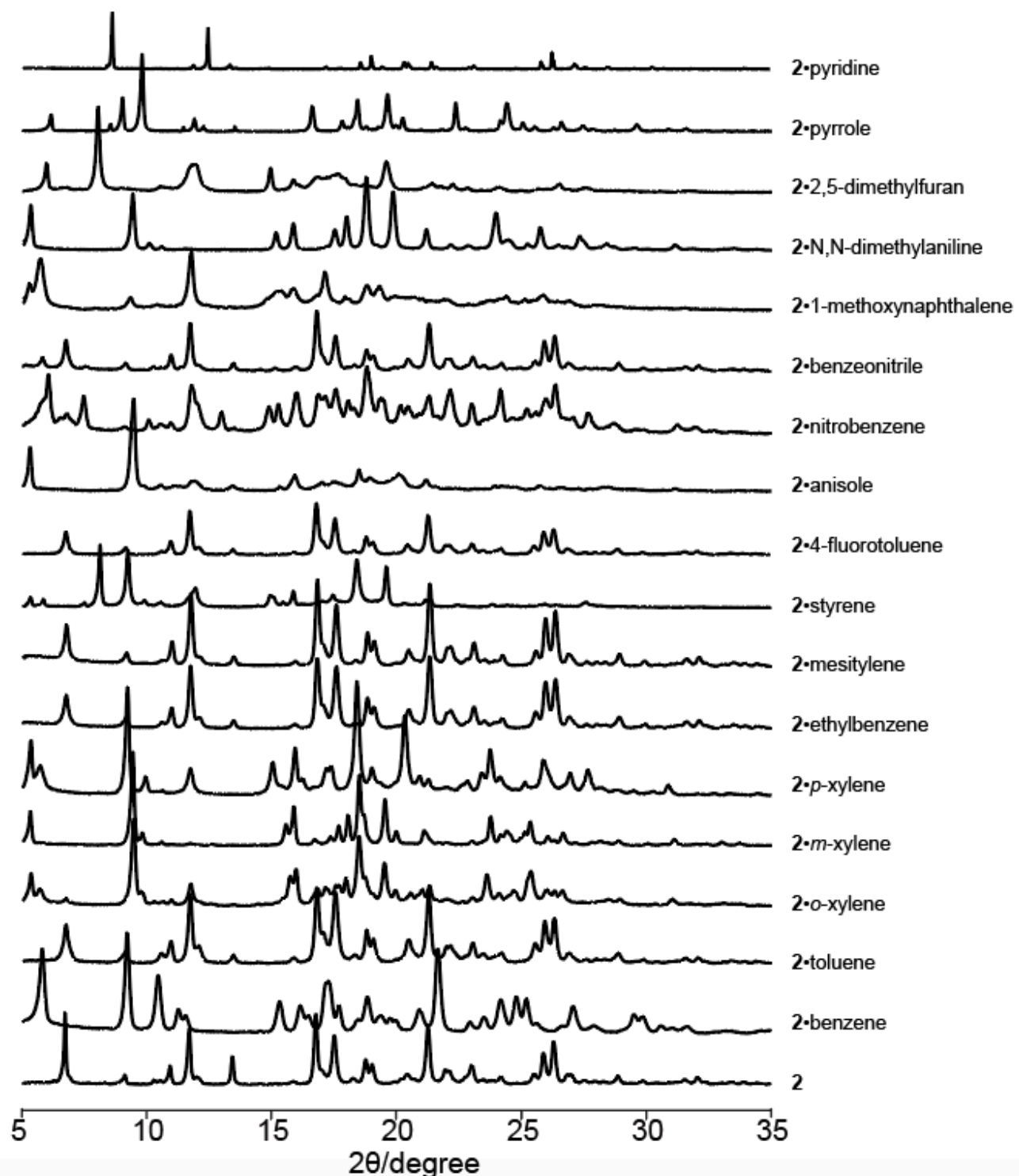


Fig. S21 PXRD 2 and 2•guest.

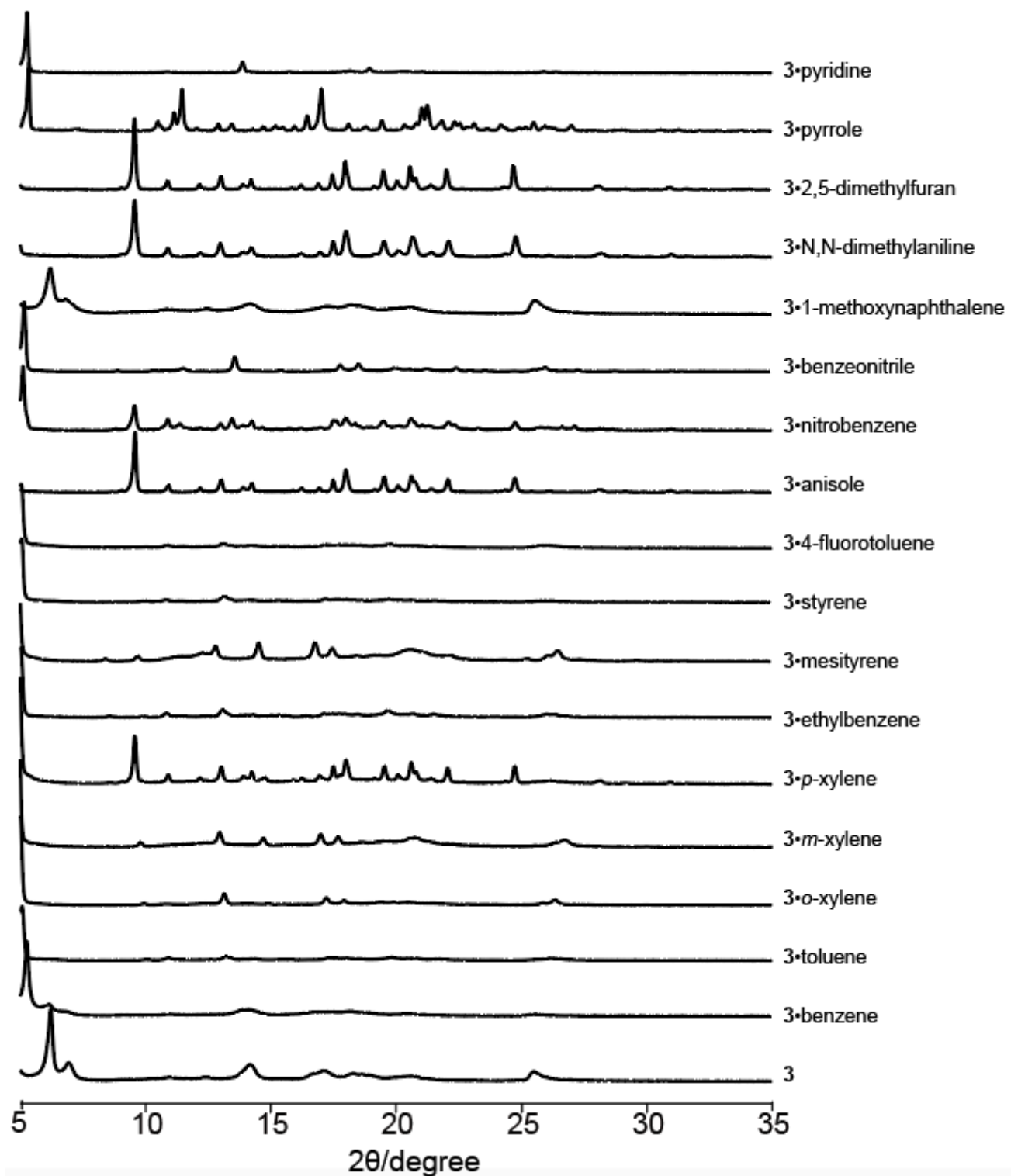


Fig. S22 PXRD 3 and 3•guest.

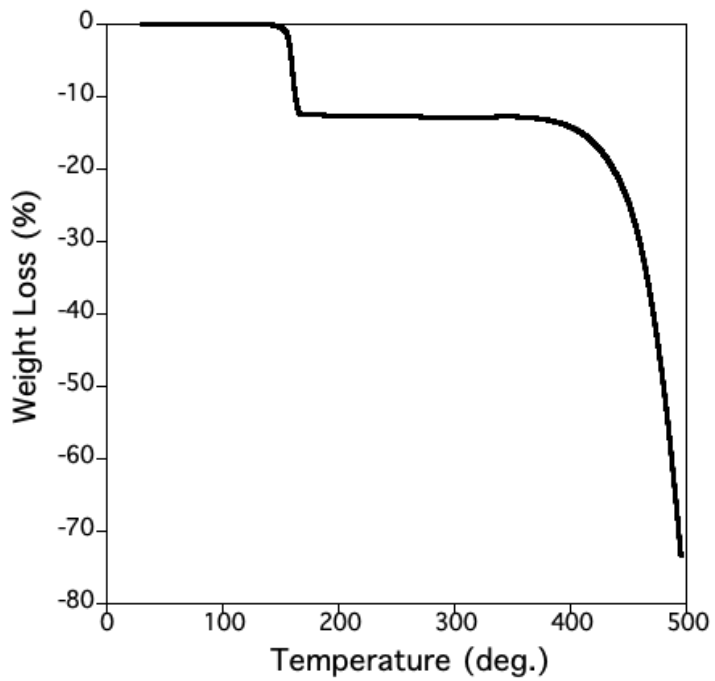


Fig. S23 TG of **1** in toluene.

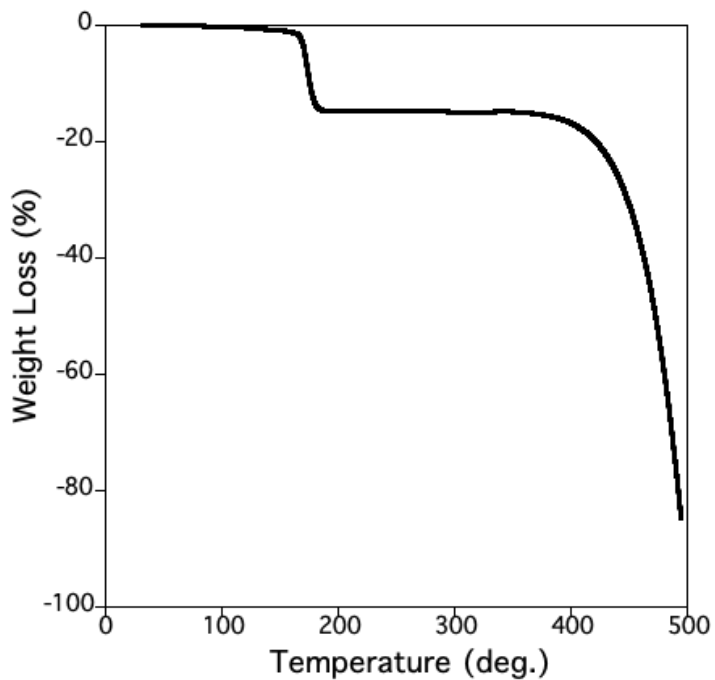


Fig. S24 TG of **1** in *p*-xylene.

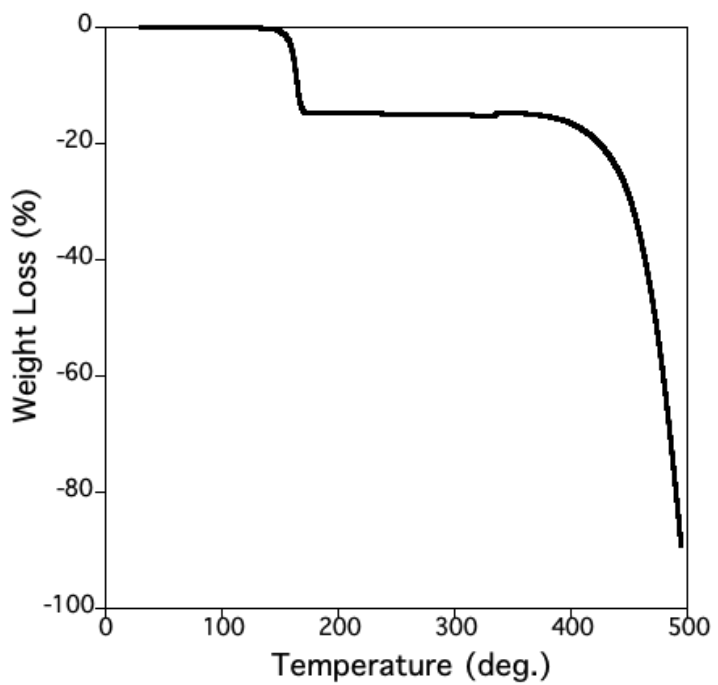


Fig. S25 TG of **1▷4**-fluorotoluene.

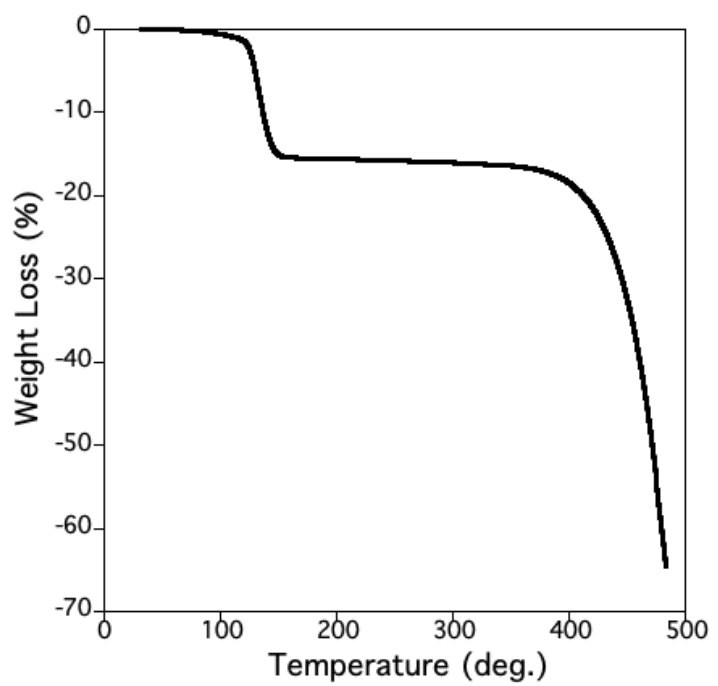


Fig. S26 TG of **1▷**anisole.

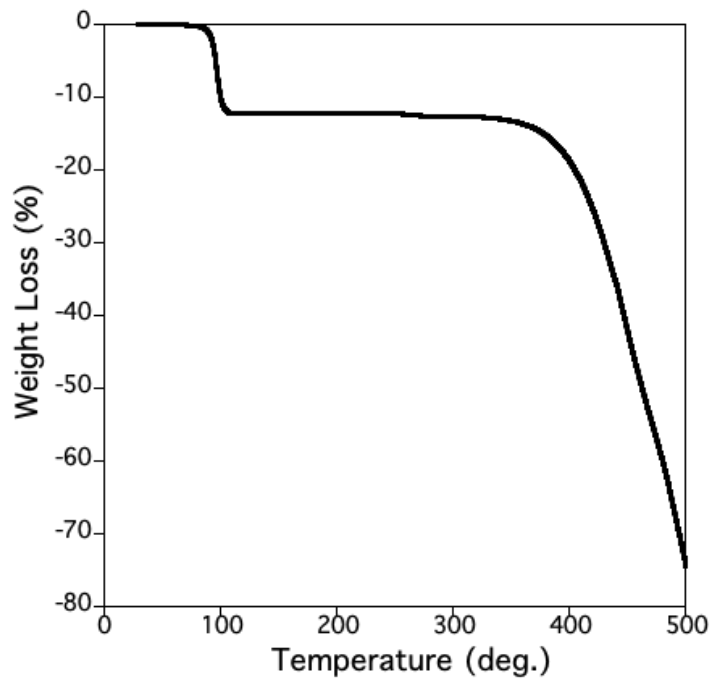


Fig. S27 TG of **2** in toluene.

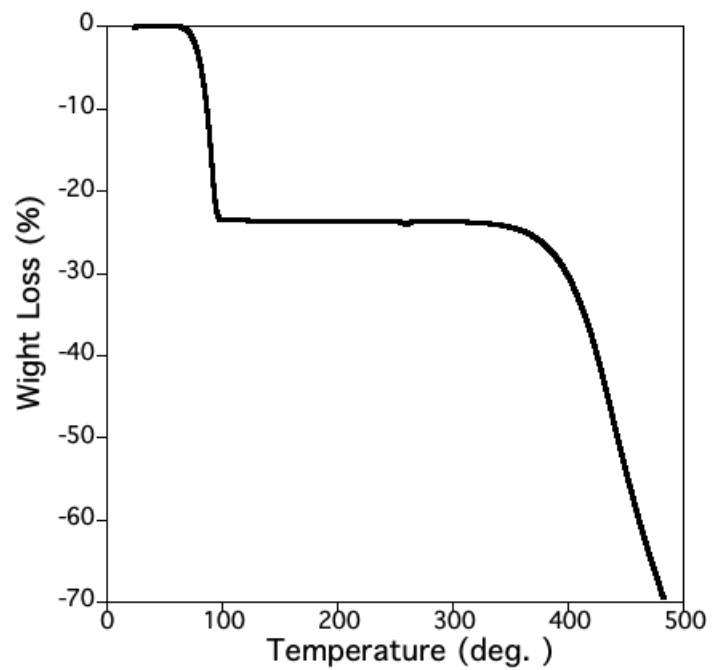


Fig. S28 TG of **2** in 2,5-dimethylfuran.

Table S2 Determination of guest molecules in various inclusion crystals.

No.	Weight loss (%)	Included guest molecules
1 •toluene	12.5	1
1 • <i>p</i> -xylene	14.5	1
1 •4-fluorotoluene	14.5	1
1 •anisole	15.4	1
2 •toluene	12.2	1
2 •2,5-dimethylfuran	23.5	2

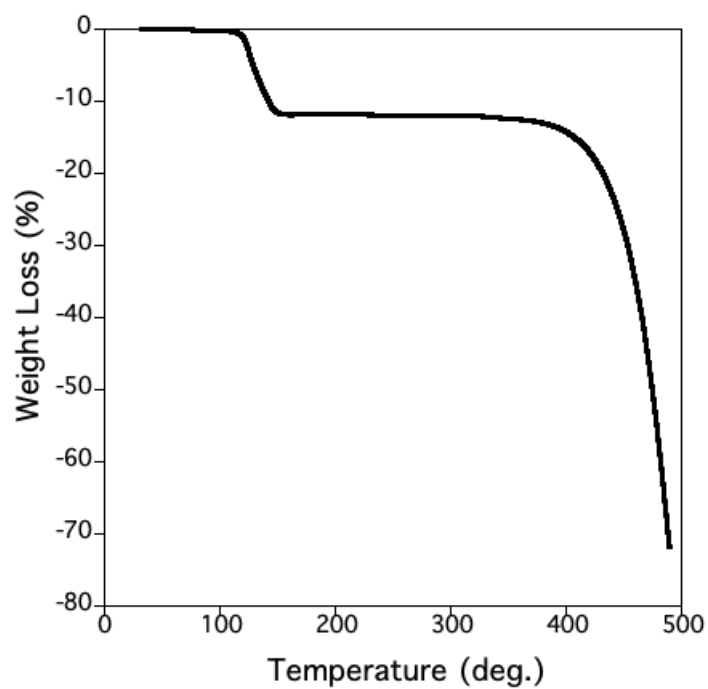


Fig. S29 TG of **1**•toluene.

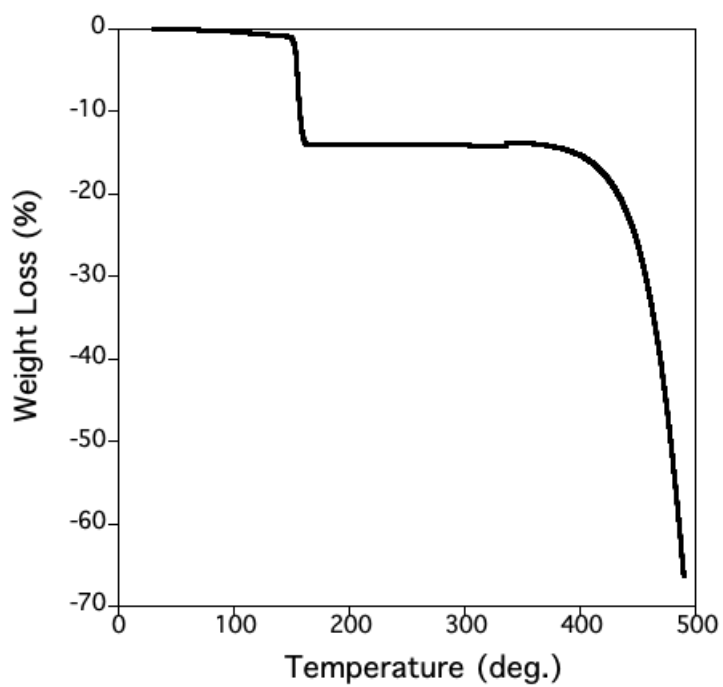


Fig. S30 TG of **1•p-xylene**.

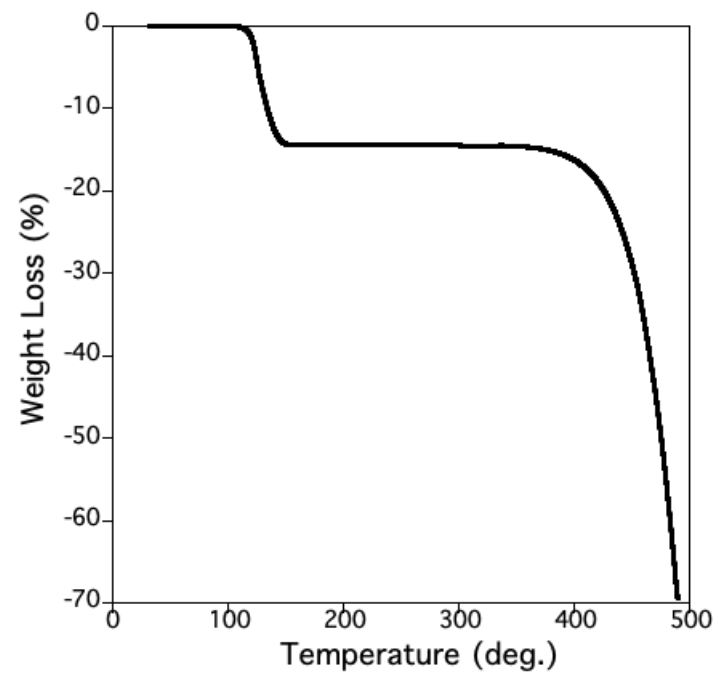


Fig. S31 TG of **1•4-fluorotoluene**.

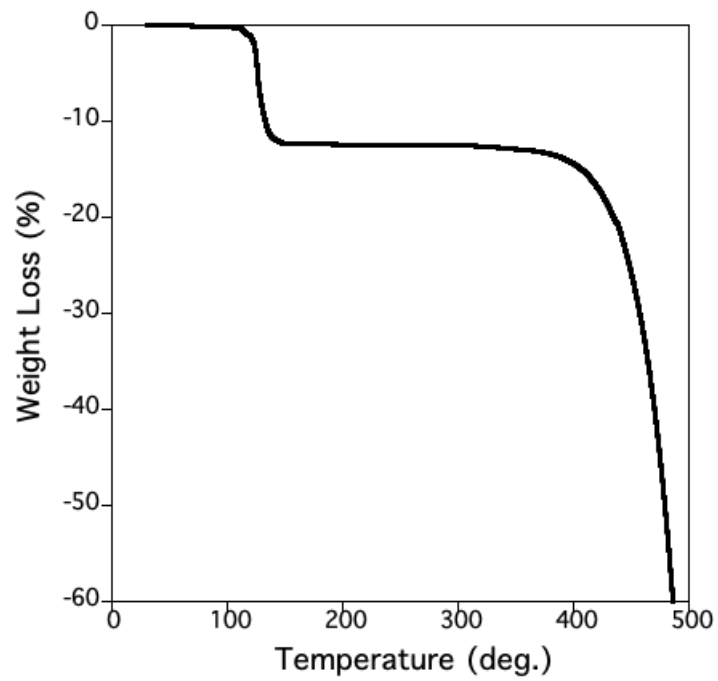
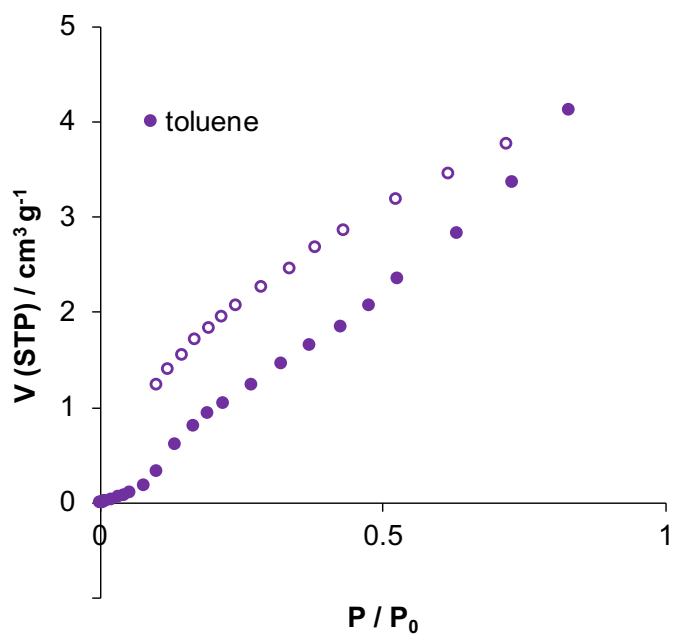


Fig. S32 TG of **1•anisole**.

(a)



(b)

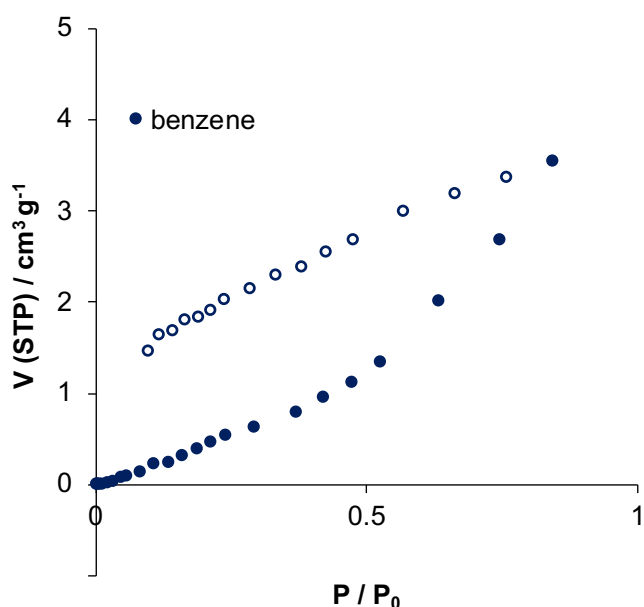


Fig. S33 Sorption isotherms of **1** toward (a) toluene and (b) benzene vapors. Solid symbols, adsorption; open symbols, desorption.

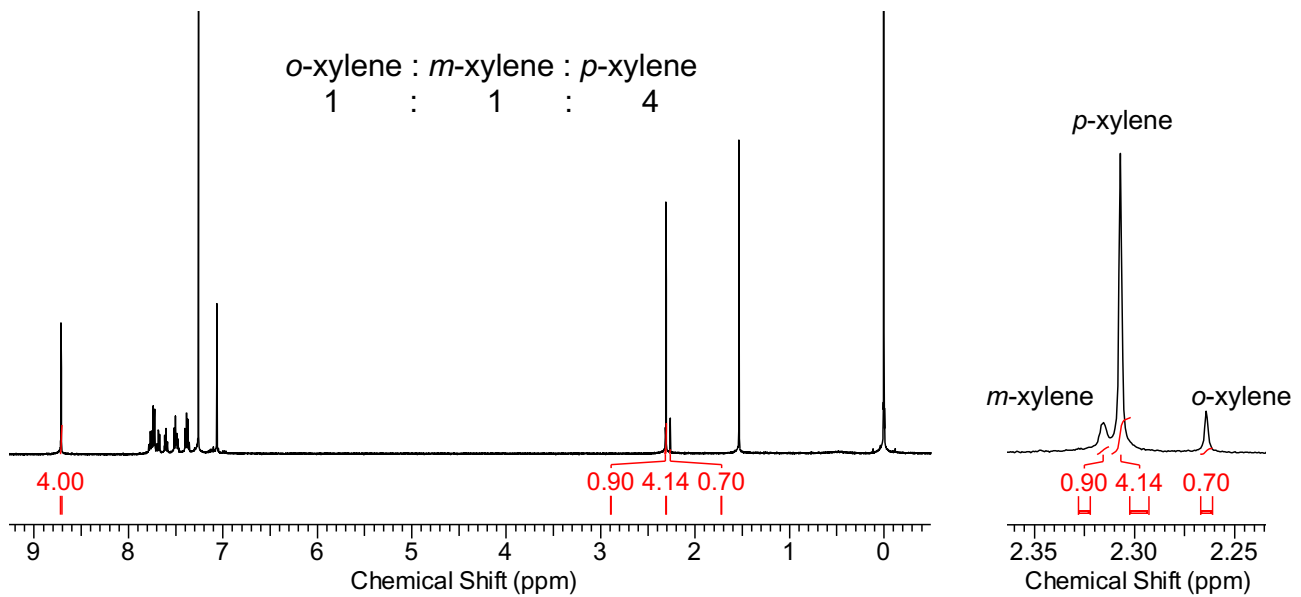


Fig. S34 Guest inclusion determined by ^1H -NMR.

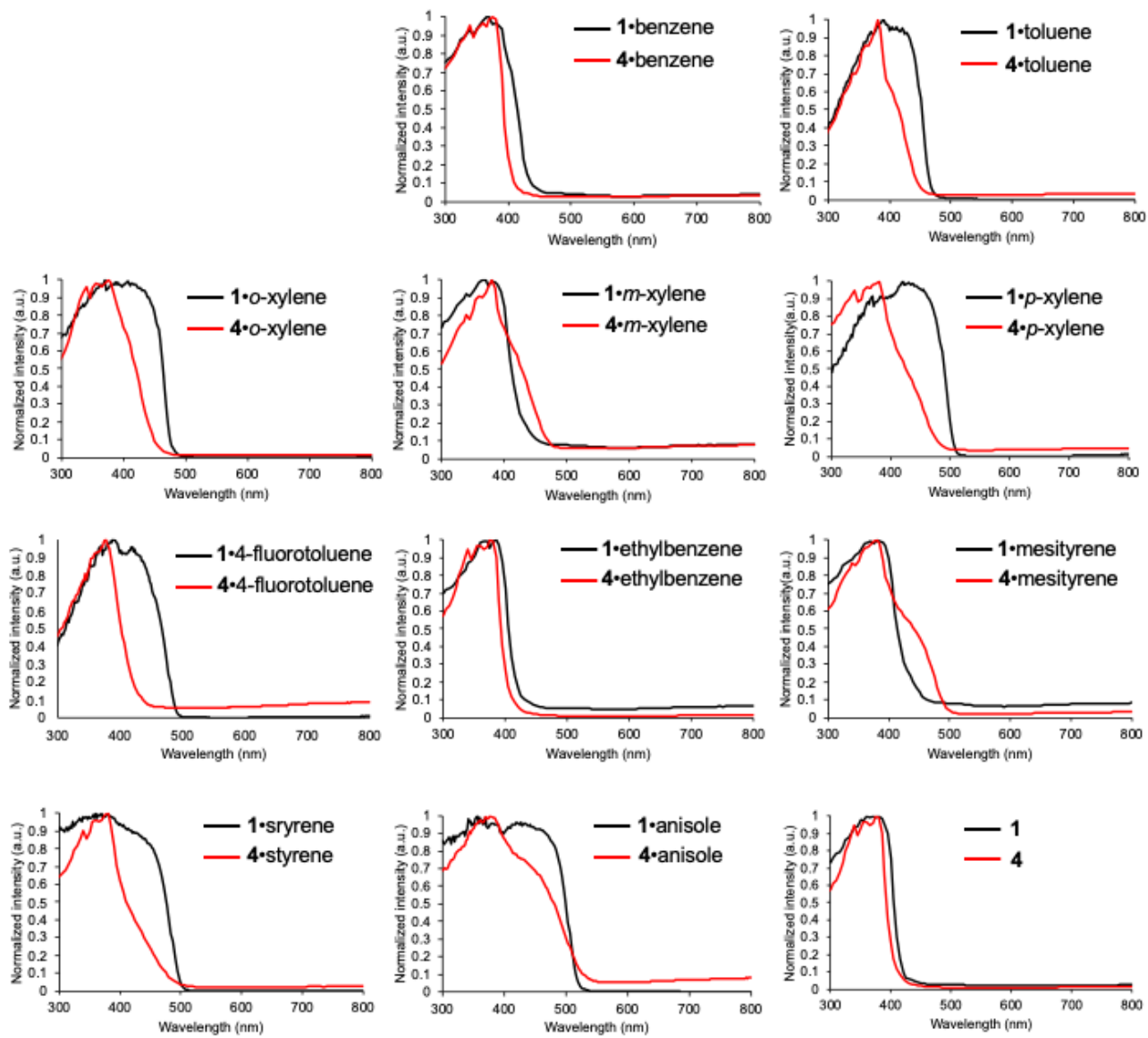


Fig. S35 Comparison of diffuse reflectance spectra of **1** and **4** with vapors.

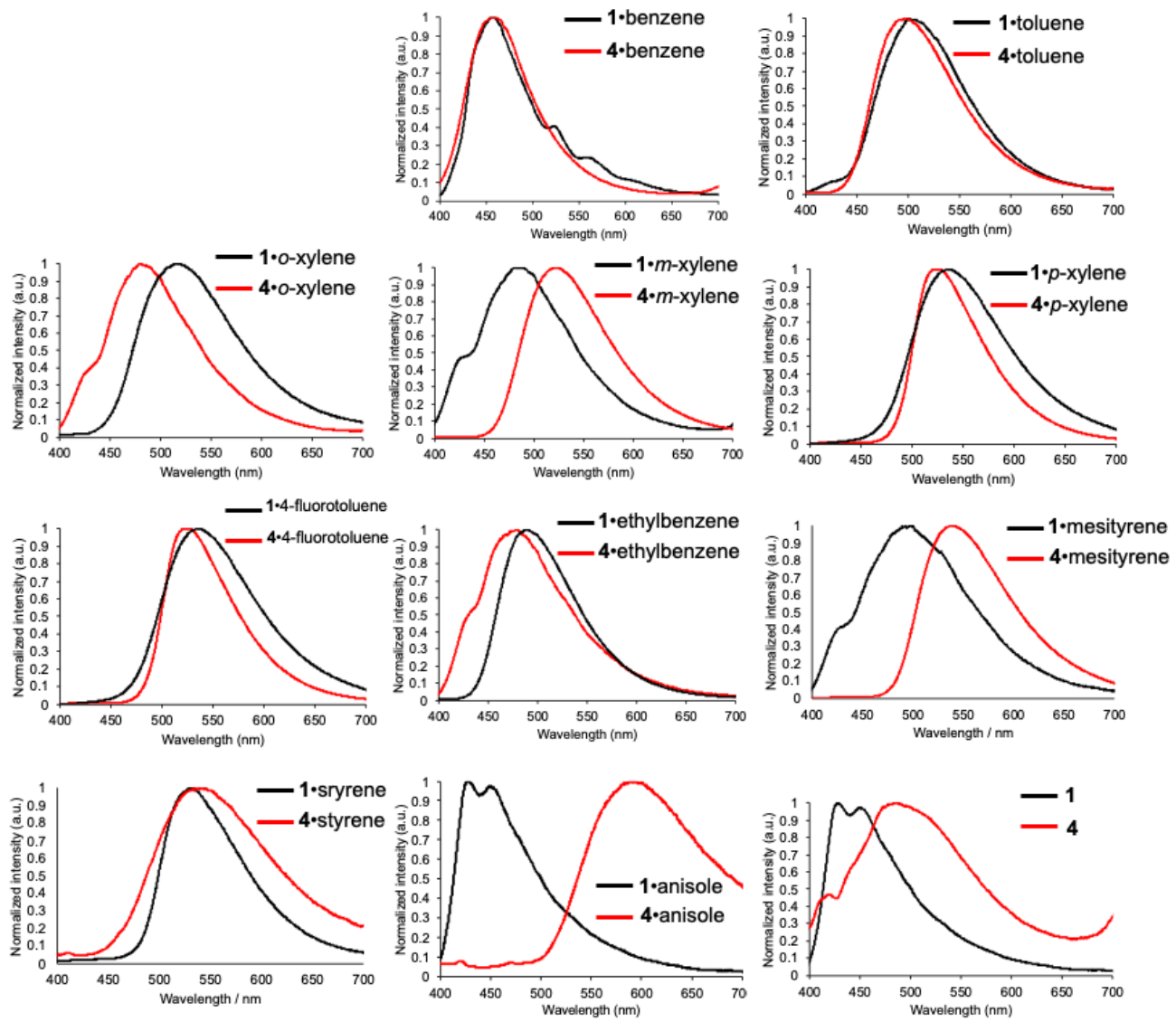


Fig. S36 Comparison of normalized emission spectra of **1** and **4** with vapors.

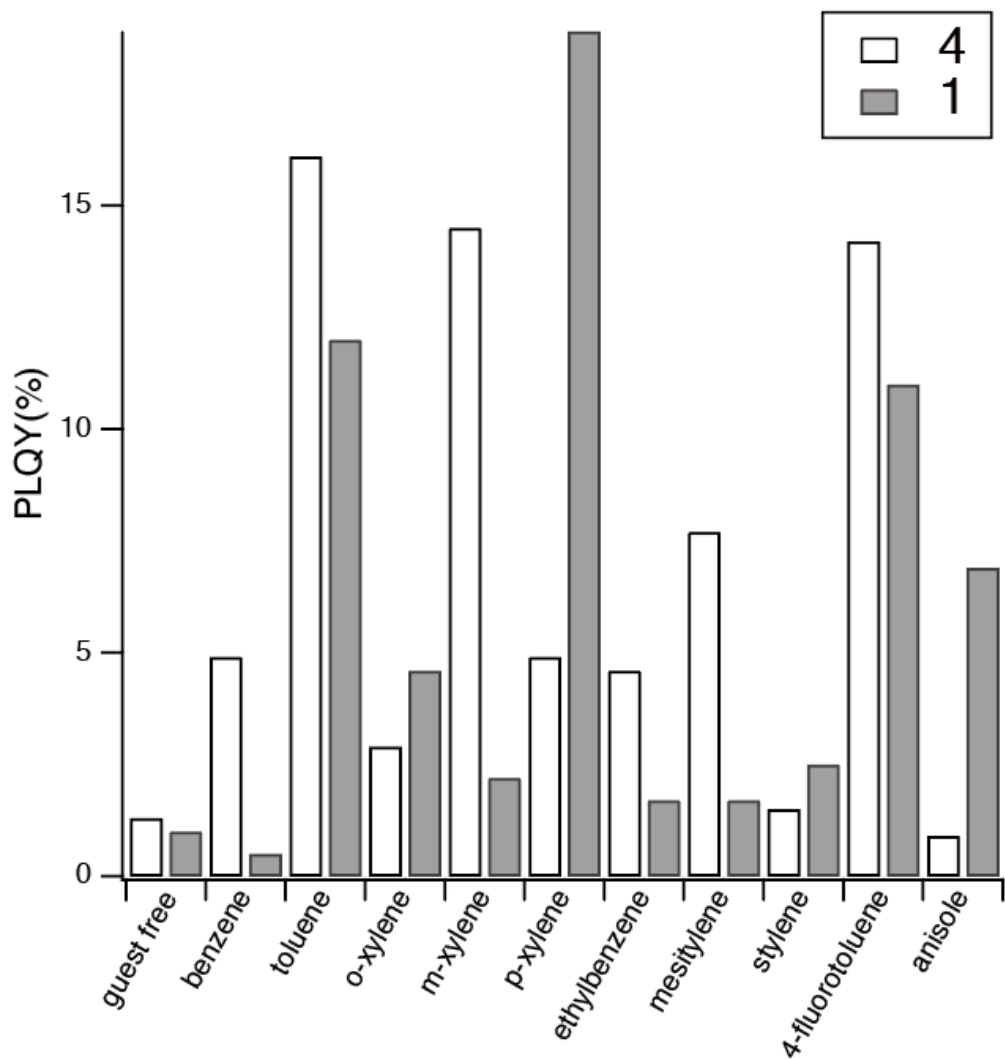


Fig. S37 Photoluminescence quantum yields of **1**, **4**, **1**•guest, and **4**•guest. Excitation at 370 nm.

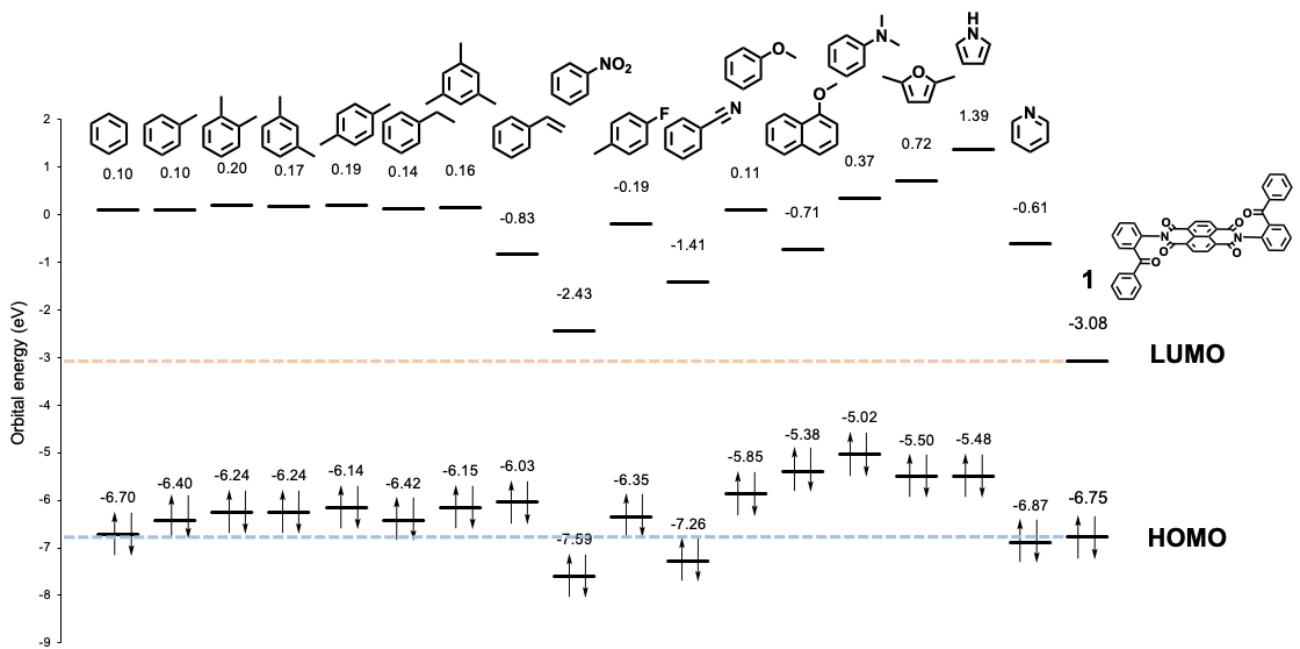


Fig. S38 Calculated HOMO-LUMO levels of the guest molecules and **1**. DFT calculations were performed using B3LYP/6-31G(d) level.

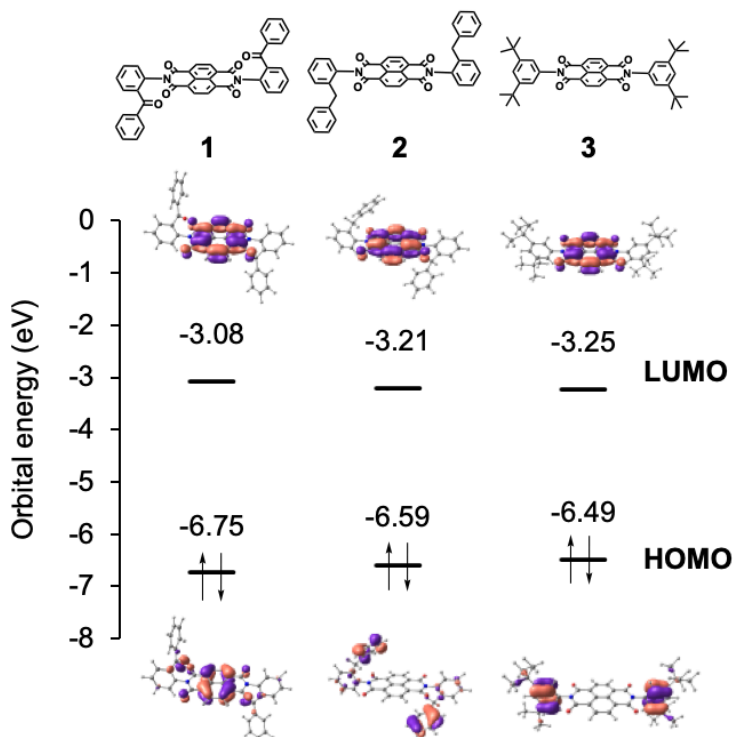


Fig. S39 Calculated HOMO-LUMO levels of **1-3** (orbital contour value 0.036). DFT calculations were performed using B3LYP/6-31G(d) level.